Establishment of the mathematical model for diagnosing the engine valve faults by genetic programming

Wen-xian Yang

Institute of Vibration Engineering, Northwestern Polytechnic University,

Xi'an, 710049, China

(*permanent address*)

Applied Mathematics & Computing Group, Department of Process and Systems

Engineering, Cranfield University, Cranfield, MK43 0AL, UK

(*present address*)

Email: w.yang@cranfield.ac.uk

Abstract Available machine fault diagnostic methods show unsatisfactory performances on both on-line and intelligent analyses because their operations involve intensive calculations and are labour intensive. Aiming at improving this situation, this paper describes the development of an intelligent approach by using the Genetic Programming (abbreviated as GP) method. Attributed to the simple calculation of the mathematical model being constructed, different kinds of machine faults may be diagnosed correctly and quickly. Moreover, human input is significantly reduced in the process of fault diagnosis. The effectiveness of the proposed strategy is validated by an illustrative example, in which three kinds of valve states inherent in a six-cylinders/four-stroke cycle diesel engine, i.e. normal condition, valve-tappet clearance and gas leakage faults, are identified. In the example, 22 mathematical functions have been specially designed and 8 easily obtained signal features are used to construct the diagnostic model. Different from existing GPs, the diagnostic tree used in the algorithm is constructed in an intelligent way by applying a power-weight coefficient to each feature. The power-weight coefficients vary adaptively between 0 and 1 during the evolutionary process. Moreover, different evolutionary strategies are employed respectively for selecting the diagnostic features and functions, so that the mathematical functions are sufficiently utilized and in the meantime, the repeated use of signal features may be fully avoided. The experimental results are illustrated diagrammatically in the following sections.

Keywords Genetic programming, Engine valve, Fault diagnosis, Immigration operator.

1. Introduction

Many mechanical fault-diagnosing techniques based on vibration analysis have been fully developed over the last few decades [1]. Among them the well-known Fast Fourier Transform (FFT) is one of the most widely used and well-established methods. Based on the FFT, Qu *et al.* [2] developed an effective tool namely the Holospectrum for diagnosing rotating machinery and Yang *et al.* [3] successfully applied it to the diagnosis of a cracked rotor; Unfortunately, the FFT-based methods failed to deal with non-stationary signals. Therefore, some time-frequency analysis methods such as Short Time Fourier Transform (STFT) [4], Wigner-Ville Distribution (WVD) [5], Wavelet Transform (WT) [6] and the Instantaneous Power Spectrum (IPS) [7] were proposed and thereafter, their improved versions were further developed [8, 9]. But few of them can meet the practical requirements completely with respect to on-line and intelligence performances because their operation needs human input and involve intensive calculations. For instance, the vibratory orbit of a rotor provides a useful clue for diagnosing the faults occurring in rotor-bearing system, but current computer programs cannot easily distinguish the orbit shapes automatically. Likewise, when diagnosing the faults in a rolling-element bearing, the quasi-periodic interval between neighbouring impulses in the signal is a very important indication that characterises the type of bearing fault. But its automatic identification is also not easily programmed into a computer. In most cases, both the shape of rotor vibratory orbit and the aforementioned quasi-periodic interval in bearing signal are estimated by the means of visual observation or manual measurement. Sometimes, however, manual methods cannot work effectively, in particular, when diagnosing the machinery with complex structures such as diesel engines. In these cases, the vibratory features

characterizing different kinds of faults overlap together, so that engineers cannot diagnose the faults at all from the direct observation of the signals. In order to tackle this difficulty in the diagnosis of faults inherent in complex machinery, an intelligent approach has been developed in this study using the Genetic Programming (abbreviated as GP) method.

The GP was first clearly defined by Koza [10]. It involves finding both the functional form (the structure of the tree) and the numeric coefficients (terminals) for the model. In comparison with the conventional Genetic Algorithm (GA) [11], its individual components part are represented by binary trees and terminals rather than by coded strings of numbers. As GP allows the optimization of much more complex structures, it can therefore be applied to a greater diversity of problems [12,13,14]. Recently, Chen *et al.* [7] adopted it to diagnose the faults occurring in rolling-elements bearings. However, most of available GPs use a few predefined binary tree structures and a small number of basic mathematical operators (e.g. +, -, $\times$, $\div$ and power). Moreover, every terminal plays an equal role in the model. This is not true in reality and affects the flexibility of the optimisation. In view of the aforementioned insufficiencies of existing GPs, a new GP approach is proposed in this paper. Using this proposed GP approach, many more mathematical functions, instead of the basic operators, will be introduced and the diagnostic tree will be constructed intelligently by applying an adaptive power-weight coefficient to each terminal (i.e. signal features). The structure of the tree is optimised adaptively with the variation of the power-weight coefficients between 0 and 1. In addition, different evolutionary strategies will be employed respectively for the selections of the functions and signal features, so that the designed functions may be sufficiently utilized whilst in the meantime, the repeated use of signal features can be completely avoided. A group of

constant numbers will be employed to avoid the occurrence of morbid solutions. In the paper, the effectiveness and feasibility of the proposed approach will be verified by an example where a mathematical model has been designed to diagnose the running states of an exhaust valve in a six-cylinders/four-stroke cycle diesel engine. The remaining parts of the paper are organized as follows.

In Section 2, the characteristics of both the vibratory signals collected from the exhaust valve and the corresponding cylinder pressure signals are analysed, based on which 8 signal features are considered to be the possible terminals of the diagnostic tree. Moreover, the same number of power-weight coefficients are designed simultaneously, from which the importance of the role of every feature in the mathematical model is indicated.

In Section 3, the 22 mathematical functions or 'operators' are deliberately designed for constructing the diagnostic tree. In the meantime, the same number of constants are used in order to avoid the occurrence of morbid solutions (e.g. the quantity in the model is divided by zero).

In Section 4, the fitness function that drives the evolutionary process is designed. Meanwhile, different evolutionary strategies are applied to the selections of the features, the 'operators' and the power-weight coefficients as well as the constant numbers, respectively.

In Section 5, using the specially designed GP program, the diagnostic tree is optimised adaptively until either the pre-defined maximum iteration time is reached or the satisfied fitness value is achieved. The optimised diagnostic tree is eventually formulated into a mathematical equation.

Finally, the effectiveness of the mathematical model identifying the running states of an engine valve is demonstrated by an illustrative experiment in Section 6.

2. Characteristics of engine signals

Nowadays, the need to further improve the diagnostic technique of engine faults has been widely recognized, but due to the complex structure and the presence of multi-excitation sources, the vibratory signals collected from engines are complicated in composition. Moreover, the features of the signals collected in different fault conditions often overlap together with each other. Thus, the engine faults are very difficult to diagnose by convenient means. Fig.1 shows the vibratory signals collected from an exhaust valve of a six-cylinders/four-stroke cycle diesel engine. The valve works under three different conditions, (1) the normal condition, (2) the valve-tappet clearance faulty condition and (3) the gas leakage fault condition. The normal valve clearance is 0.1mm and in the experiments, a severe valve clearance fault was simulated and the clearance was adjusted to be 0.5mm. The gas leakage fault was simulated by producing a 3mm long crack on the cap of the valve. Two kinds of signals were considered in the calculation, one was the vibration signal collected from the cap of the exhaust valve; another was the cylinder pressure signal collected from a standard Thompson adapter that was positioned between the indicator cock and the cylinder head. The sampling frequency was 25 kHz and during the data acquisition process, the rotating speed of the engine was kept at a constant 1500 rpm.

From Fig.1, it was found that the signals collected under different valve running conditions showed different complexities in structure. But the signal at every stage appeared similarly in the form of the impulses with decaying amplitudes and periods, despite the running states of the valve. Among the five stages, the fourth stage showed the strongest vibration. Moreover, the vibration at each stage increased or decreased more or less when the valve worked abnormally. Based on these observations the

following criteria were designed for characterising the signals. If it was assumed that the time series signal is x_i (i=1, 2, …, N), then

(1) General vibration intensity E_1

$$E_1 = \sqrt{\sum_{i=1}^{N} x_i^{\,2} / N} \tag{1}$$

Where, N denotes the number of data.

(2) Vibration intensity at the second stage E_2

$$E_2 = \sqrt{\sum_{i=l}^{m} x_i^{\,2} / (m - l + 1)} \tag{2}$$

Where l and m indicate the first and the last number of data collected at the second stage, respectively.

(3) Vibration intensity at the third stage E_3

$$E_3 = \sqrt{\sum_{i=m+1}^{n} x_i^{\,2} / (n - m + 2)} \tag{3}$$

Where n indicates the last number of data collected at the third stage.

(4) Structural complexity S

$$S = -\sum_{i=1}^{\Omega} \frac{N_i^{'}}{N} \log_2 \left(\frac{N_i^{'}}{N} \right) \tag{4}$$

Where S, in essence, is the structural entropy of the signal. Herein, the amplitude region of the signal is divided into Ω sub-regions. $N_i^{'}$ indicates the number of the data located in the i-th sub-region.

From the long-term observations, it was also found that the vibratory energy of the valve was redistributed in the frequency domain when the valve worked abnormally, as shown in Fig.2. It is necessary to note that the subplots in Fig.2 are the frequency spectra of those signals shown in Fig.1.

From Fig.2, it was observed that when the valve worked abnormally, the vibration energy moved forward towards the high frequency region (i.e. larger than 9kHz) and in consequence, the low frequency vibration decreased correspondingly at the same time. The observation showed that the remarkable differences among the spectra occurred in the regions (6.5kHz, 9kHz) and (9kHz, 12.5kHz), respectively. In order to characterize these phenomena, the fifth and the sixth criteria were designed.

(5) The ratio of the vibration in the region from 6.5kHz to 9kHz, R_1

$$R_1 = \frac{\sum_{i=a}^{b} d_i}{\sum_{j=1}^{N} d_j} \tag{5}$$

Where $d_j\,(j = 1,2,\cdots,i,\cdots,N)$ are the spectral data derived by the FFT, and a and b represent the first and the last number of spectral data in the region (6.5kHz, 9kHz), respectively.

(6) The ratio of the vibration in the region from 9kHz to 12.5kHz, R_2

$$R_2 = \frac{\sum_{i=b}^{N} d_i}{\sum_{j=1}^{N} d_j} \tag{6}$$

In order to see whether or not these vibratory criteria can really work in identifying the running states of the valve, Fig.3 plots, their calculated results were obtained during a series of experiments.

From Fig.3, it was found that the vibratory criteria, derived under different valve running conditions, either overlapped together or were very close to each other. Obviously, they cannot be directly applied to the identification of valve states, but from eqns. (1) to (6), it is seen that these criteria are much more easily obtained than those used by [7].

Experiments revealed that the cylinder pressure was also a very important feature for diagnosing the valve states, as shown in Fig.4. From this figure, it is clearly seen that when the running state of the valve has changed especially when a gas leakage fault occurs, the maximum value of the cylinder pressure will change significantly. Moreover, the decreasing ratio of the cylinder pressure in one working cycle is modified as well.

Based on the observations shown in Fig.4, the following seventh and the eighth features were further designed.

(7) The maximum cylinder pressure $P_{\max}$

$$P_{\max} = \max(p_i \mid i = 1,2,\cdots,M) \tag{7}$$

Where M indicates the number of data included in the cylinder pressure signal $p_i(i = 1,2,\cdots,M)$.

(8) The decreasing ratio R_{p} of the cylinder pressure signal

$$R_{\mathrm{p}} = \frac{\Delta P}{P_{\max}} \tag{8}$$

The $P_{\max}$ and ΔP are indicated in Fig.5. Their calculation results derived during experiments are shown in Fig.6.

From Fig.6, it is seen that the $P_{\max}$ derived under different valve conditions overlap together with each other and so does the R_{p}. From the calculated results, shown in Figs.3 and 6, it can be concluded that the valve states cannot be identified correctly by directly using the calculated results of these criteria. This is why a new approach has been developed and described in this paper.

Using the aforementioned 8 signal features criteria, the set of features for constructing the diagnostic tree is written as a 3×8 matrix **F**=[$\mathbf{E}_1$, $\mathbf{E}_2$, $\mathbf{E}_3$, **S**, $\mathbf{R}_1$, $\mathbf{R}_2$, $\mathbf{P}_{\max}$, $\mathbf{R}_{\mathrm{p}}$]. Where, $\mathbf{E}_1 = [E_1^{'} \quad E_1^{''} \quad E_1^{'''}]^{'}$. $E_1^{'}$, $E_1^{''}$ and $E_1^{'''}$ are the E_1 respectively

derived under three different kinds of valve states. The other features in the matrix **F** have the similar expressions.

In addition, the research carried out in [15] reveals that different signal features play different roles in fault diagnosis. In other words, some features play more important roles, while the others play less important roles or even, in some cases, do not play any role in the diagnosis. In view of this, a particular set of power-weight coefficients $\mathbf{C}=\{0 \le c_i \le 1 \mid i=1,2,\cdots,8\}$ was further designed. They corresponded to the aforementioned 8 signal feature criteria, and indicate the roles that these criteria play in the construction of the diagnostic tree. With the aid of **C**, the flexibility of the optimisation of the diagnostic tree can be dramatically improved. For example, in case of $c_i = 0$, the *i*-th feature in the set of terminals **F** does not play any role in the tree, so the binary tree related to this feature can be cut off from the main trunk. Conversely, the binary trees related to those features with $c_i \neq 0 (i=1,2,\cdots,8)$ will be reserved.

3. Mathematical functions

Instead of using a few basic operators adopted by conventional GPs, a series of mathematical functions are taken as the 'operators' in the proposed GP so that more complex mathematical computation forms can be involved in the optimisation process. The designed 'operators' are listed in Table 1.

In the functions, y_j is the result derived from the *j*-th iterative calculation. f_i represents the *i*-th feature in the set of terminals **F**. c_i denotes the power-weight coefficient corresponding to f_i. In addition, a group of constant numbers $\varepsilon=\{0 < \varepsilon_i \le 1 \mid i=1,2,\cdots,8\}$ was also designed for avoiding the occurrence of morbid

solutions. The coded constant numbers in the set ε_i (i=1,2,…,8) can be optimised as well. From Table 1, it should be noticed that in designed 'operators', the feature f_i is multiplied by the power-weight coefficient c_i first before carrying out further calculations of the function, so that the roles of the features play in the mathematical model are taken into account in the calculation. Moreover, through optimising c_i (i=1,2,…,8), the structure of the diagnosing tree may be optimised adaptively whilst in contrast, the convenient GPs do not posses this merit. The diagram of the diagnostic tree is shown in Fig.7.

In this figure, the composite criterion w is finally derived from the diagnostic tree, which can be taken as the measure for identifying the running states of the valve.

4. Evolutionary strategies

During the evolutionary process, four factors will be involved in the optimisation. They are the order of the features in the set **F**, the coded coefficients in the set **C**, the coded constant numbers in the set $\boldsymbol{\varepsilon}$ as well as the order of the functions in the set of 'operators', respectively. For the last three factors, their evolution will be realized by performing the conventional crossover and mutation operations. The details of the crossover and mutation operations may be found from [11]. But the optimisation of the order of the features in **F** cannot be manipulated in the same way, otherwise the features in the set **F** could be used repeatedly. In essence, the optimisation of the order of the features in **F** belongs to the type identified as Travelling Salesman Problems (TSPs). The related description about the TSPs may be found in [16]. Whilst aiming at solving the TSPs by using genetic algorithms, the author has been innovative and

proposed an improved genetic operator namely ‘Immigration Operator (IO)’ [17]. A brief introduction of the IO is given as follows.

The IO is a special strategy for generating individuals at the outside of the population and then introducing the fitter ones into the population to substitute for those inferior individuals. The operating scheme of the IO is depicted in Fig. 8. Where, M represents the scale of the population, $P_{\text{immigration}}$ the probability of immigration operation, I the number of individuals that will be generated, f_i the fitness value of the i-th individual, f_{mean} the mean fitness of the individuals contained in present population.

As depicted in Fig.8, the individuals are generated stochastically, but the population will not accept all individuals being generated. Only those with the fitness larger than the mean fitness of the available individuals contained in present population may be regarded as the “qualified ones”. Hence, the individuals accepted by the population posses better fitness. This is why the IO can drive the evolution of the population more successfully. The other merits of the IO may be found from [17].

Using the different evolutionary strategies, the operating diagram of the GP is drawn in Fig.9.

In order to accomplish a perfect classification of different valve states, both the largest pseudo space distances among different groups of samples and the smallest pseudo space distances among different samples contained in the same group are considered simultaneously. The fitness function for the GP is designed as

$$f = \frac{\sum_{j,k=1,j\neq k}^{a}\left[\sum_{i,l=1}^{b}\left(w_{ij}-w_{lk}\right)\right]}{\sum_{k=1}^{a}\left[\sum_{i,l=1,i\neq l}^{b}\left(w_{ik}-w_{lk}\right)\right]} \tag{9}$$

Where *a* indicates the number of valve states being considered, *b* the number of data included in the signal. w_{ij} denotes the composite criterion derived from the *i*-th signal collected under the *j*-th running state of the valve. w_{lk} and w_{ik} have the similar meanings.

5. The implementation of the GP

Adopting the GP algorithm depicted in Fig.9 and taking the fitness function *f* described by eqn. (9) as the measure for evaluating the fitness levels of the individuals. The diagnostic tree, shown in Fig.7, is optimised for diagnosing three such kinds of valve running states as (1) the normal condition, (2) the valve-tappet clearance fault and (3) the gas leakage fault. The recorded evolutionary history is shown in Fig.10.

The optimised results are listed in Table 2.

After substituting the optimised results listed in Table 2 into the diagnostic tree, the following mathematical model for identifying the valve state is readily derived.

$$w = \frac{0.6745^2 \times R_{\mathrm{p}} \times P_{\max}}{0.5746 + 0.0515 \times S + \left[\left| \dfrac{0.1540 \times R_1}{0.0279 + \left(\left| \dfrac{\left|0.5351 \times R_2 / 0.6619\right|^{1/2} - 0.0212 \times E_2}{0.9965 + 0.6745 \times E_3} \right| \right)^{1/2}} \right|\right]^{1/2}}$$

$$= \frac{0.4550 \times R_{\mathrm{p}} \times P_{\max}}{0.5746 + 0.0515 \times S + \left[\left| \dfrac{0.1540 \times R_1 \times \left|0.9965 + 0.6745 \times E_3\right|^{1/2}}{0.0279 \times \left|0.9965 + 0.6745 \times E_3\right|^{1/2} + \left(\left|0.8991 \times \left|R_2\right|^{1/2} - 0.0212 \times E_2\right| \right)^{1/2}} \right|\right]^{1/2}} \tag{10}$$

From equation (10), it should be noticed that only 7 features appear in the mathematical model, though 8 criteria were considered during the optimisation. This is because the first function being selected is $y_{j+1} = \sqrt{|c_i f_i y_j|}$ (refer to Tables 1 and 2). As at the beginning of the GP, the initial value of y_j is zero, this function does not play any role in the model and the role of the first feature in the optimised set **F** is ignored. From Table 2, it is found that this feature is E_1. This is also why E_1 does not appear in the final mathematical model.

6. Application of the mathematical model in the diagnosis of valve states

Aiming at demonstrating the effectiveness of the derived mathematical model in identifying the running states of the valve, 29 additional signals were collected under each kind of valve running condition. After extracting the features specified by the set **F** from the sample data, the features were substituted into eqn. (10). The Composite Criterion *w* was calculated and the results plotted in Fig.11.

Fig.11 shows that using the mathematical model derived by the GP, the three different kinds of valve states are distinguished correctly and efficiently. The overlapping phenomenon among them does not occur at all on the composite criterion *w*. In order to further prove the merit of the derived mathematical model on valve state classification, the following experiments were also carried out for comparison.

The Principal Component Analysis (PCA) method has been widely accepted as a favoured tool for constructing the classification models [15]. Hence, the PCA was also employed to solve the present problem. The numerical results of the first, the

second and the third orders of principal components (PC1, PC2 and PC3) derived by the PCA are given in Fig.12.

From Fig.12, it is easily found by using the mathematical model, derived from the PCA method, that the three kinds of valve states cannot be distinguished satisfactorily because of the overlapping phenomenon existing among them. The accuracy of the classification may be improved by employing the Kernel Principal Component Analysis (KPCA) method [15], but in the case of using KPCA, the mathematical model is difficult to establish as the a non-linear operation is involved in the calculation algorithm.

7. Concluding remarks

From the aforementioned research studies, the merits of the proposed GP approach may be summarized as follows.

(1) In comparison with the features adopted by [7], the signal features used in the proposed GP are more easily obtained. ; No further complex calculation is needed;

(2) The introduction of the power-weight coefficients into the GP allows the optimisation of the diagnostic tree to be a more logical process, dramatically improving the flexibility of the optimisation;

(3) The use of different evolutionary strategies fully ensures sufficient utilization of both the signal features and the ‘operators’. Incorporating the constant numbers introduced, the morbid solutions are completely avoided;

(4) The proposed GP approach produces a simple, feasible and effective mathematical model for diagnosing the running states of the engine valve. However, such a perfect model is difficult to achieve by using the conventional

signal processing methods like wavelet transform or other advanced signal processing tools;

(5) The simple calculation of the signal features and the mathematical model make it much easier to realize an intelligent online fault diagnostic system;

(6) Compared with the PCA or other conventional classification methods, the proposed GP technique shows more powerful ability in solving the classification problems.

Acknowledgements

This research work was supported by the National Natural Science Foundation of China (Ref. No. 50205021) and the Shaanxi Provincial Natural Science Foundation (Ref. No. 2002E$_2$26). The author would like to appreciate both reviewers and Dr Mike Seymour for their kind suggestions to the paper.

References

1. Z.K. Peng, F.L. Chu, Application of the wavelet transform in machine condition monitoring and fault diagnostics: A review with bibliography, *Mechanical System and Signal Processing* 18 (2004) 199-221.
2. L.S. Qu, X. Liu, Y.D. Chen, The Holospectrum: A new method for rotating surveillance and diagnosis, Journal of Mechanical Signature and Signal Processing 3 (3) (1989) 255-268.
3. W.X. Yang, L.S. Qu, J.S. Jiang, Study of the diagnostic features of a rotor with a transverse crack, *INSIGHT-Non-Destructive and Condition Monitoring* (*The Journal of the British Institute of Non-Destructive Testing*) 43 (8) (2001) 537-545.

4. I.S. Koo, W.W. Kim, Development of reactor coolant pump vibration monitoring and a diagnostic system in a nuclear power plant, *ISA Transactions* 39 (2000) 309-316.
5. P.C. Russell, J. Cosgrave, D. Tomtsis, A. Vourdas, L. Stergioulas, J.R. Jones, Extraction of information from acoustic vibration signals using Gabor Transform type devices, *Measurement Science and Technology* 9 (1998) 1282-1290.
6. W.J. Staszewski, Structural and mechanical damage detection using wavelets, *The Shock and Vibration Digest* 30 (1998) 457-472.
7. P. Chen, M. Taniguchi, T. Toyota, Z.J. He, Fault diagnosis method for machinery in unsteady operating condition by instantaneous power spectrum and genetic programming, *Mechanical System and Signal Processing* 19 (2005) 175-194.
8. A. Francois, F. Patrick, Improving the readability of time-frequency and time-scale representations by the reassignment method, *IEEE Transactions on Signal Processing* 43 (1995) 1068-1089.
9. P.W. Tse, W.X. Yang, H.Y. Tam, Machine fault diagnosis through an effective exact wavelet analysis, *Journal of Sound and Vibration* 277 (2004) 1005-1024.
10. J.R. Koza, Genetic programming: On the programming of computers by means of natural selection, *A Bradford Book, MIT Press* (1992).
11. J. Holland, Adaptation in natural and artificial systems, *Ann Arbor*: *University of Michigan Press* (1975).
12. C.D. Stefano, A. D. Cioppa, A. Marcelli, Character preclassification based on genetic programming, *Pattern Recognition Letters* 23 (2002) 1439-1448.
13. M.L. Wong, A flexible knowledge discovery system using genetic programming and logic grammars, *Decision Support Systems* 31 (2001) 405-428.

14. P.A. Whigham, P.F. Crapper, Modelling rainfall-runoff using genetic programming, *Mathematical and Computer Modelling* 33 (2001) 707-721.
15. W.X. Yang, Vibration-based diagnosis of engine valve faults, *INSIGHT-Non-Destructive and Condition Monitoring* (*The Journal of the British Institute of Non-Destructive Testing*) 45 (8) (2003) 1-7.
16. R. Yang, Solving large travelling salesman problems with small population, *International Conference on Genetic Algorithms in Engineering Systems: Innovations and Application*, University of Strathclyde, Glasgow, UK (September 1997) 157-162.
17. W.X. Yang, An improved genetic algorithm adopting immigration operator, *International Journal of Intelligent Data Analysis* 8 (4) (2004) 385-401.

Figure Captions

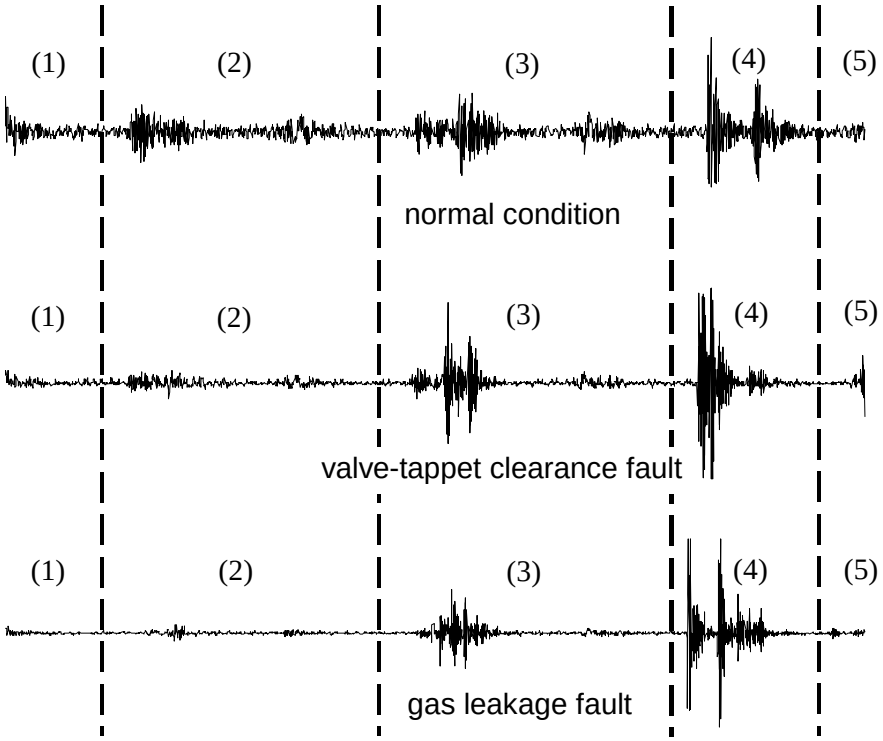

(1) the exhaust valve closes; (2) the inlet valve closes; (3) gas combustion burst; (4) the exhaust valve opens; (5) the inlet valve opens.

Fig.1 Vibration signal collected from the exhaust valve of the engine

(Drawn by W.-X. Yang)

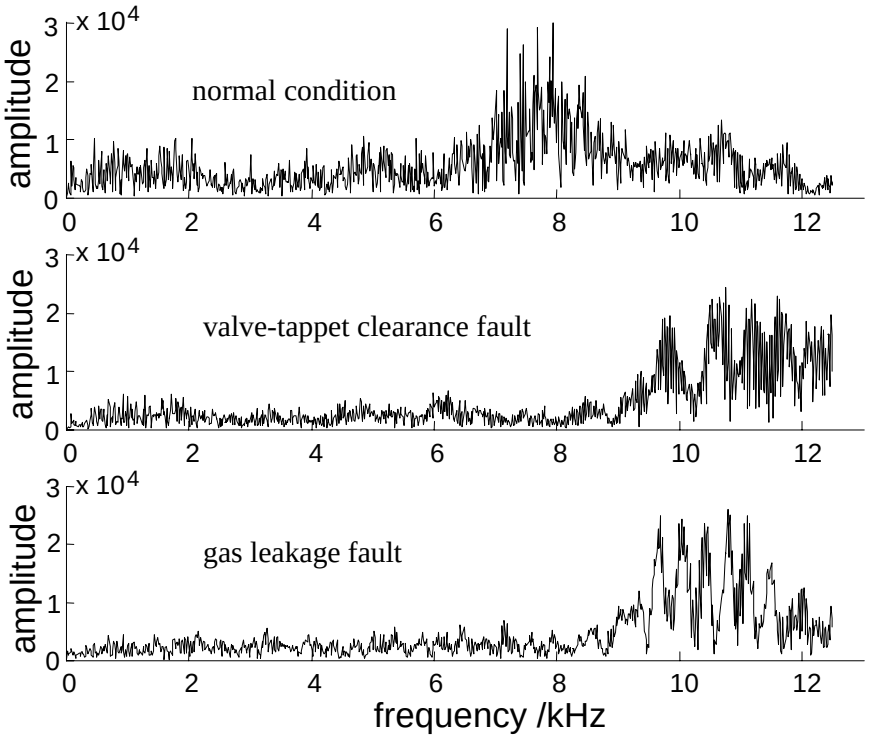

Fig.2 The frequency spectra of the signals shown in Fig.1

(Drawn by W.-X. Yang)

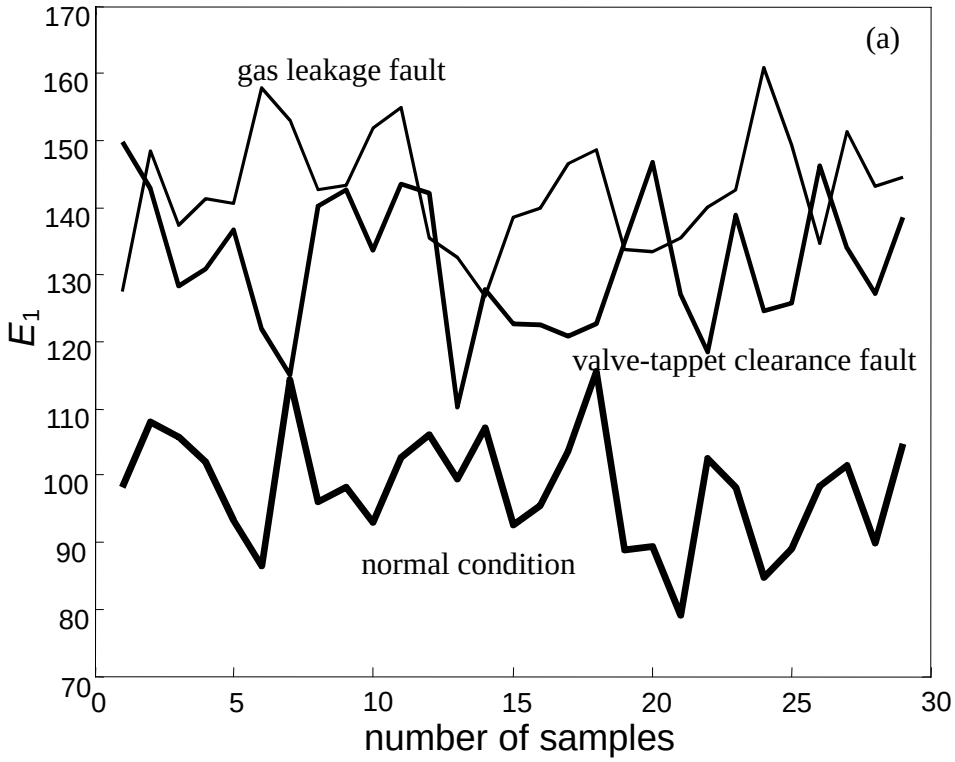
(a)
gas leakage fault
valve-tappet clearance fault
normal condition
E_1
number of samples
170
160
150
140
130
120
110
100
90
80
70
0
5
10
15
20
25
30

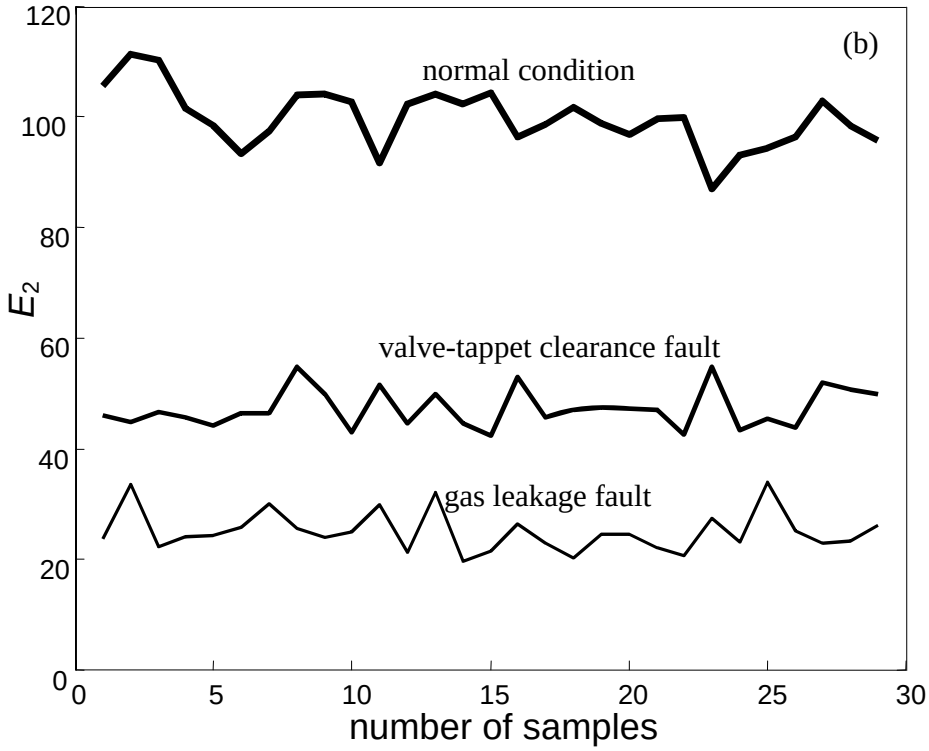
(b)
normal condition
valve-tappet clearance fault
gas leakage fault
E_2
number of samples
120
100
80
60
40
20
0
0
5
10
15
20
25
30

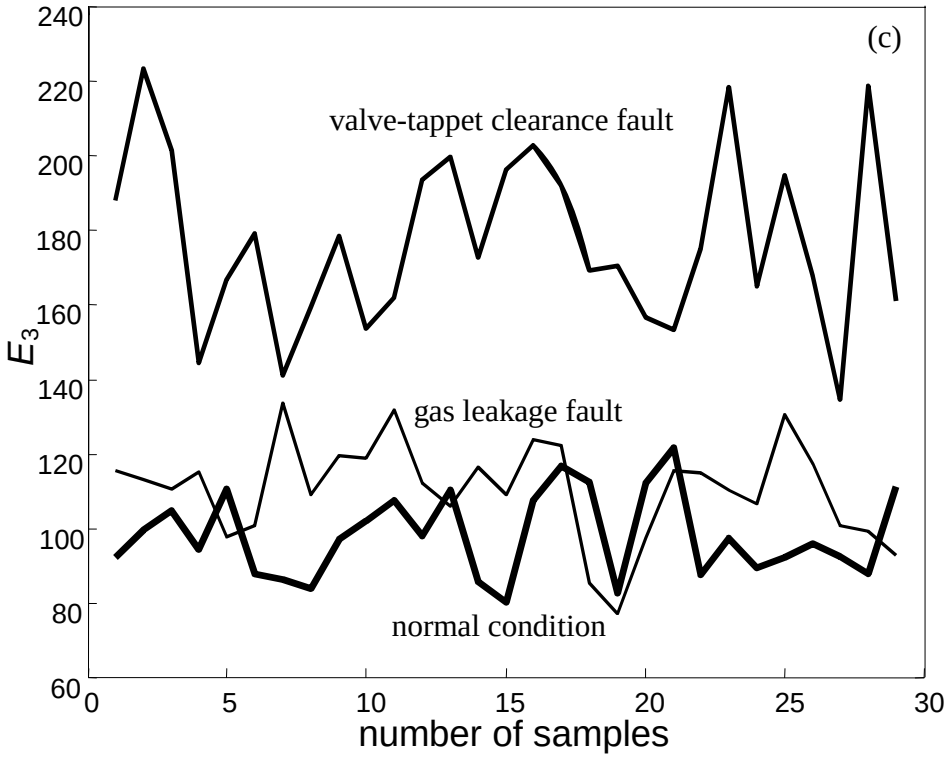
(c)
valve-tappet clearance fault
gas leakage fault
normal condition
E_3
number of samples

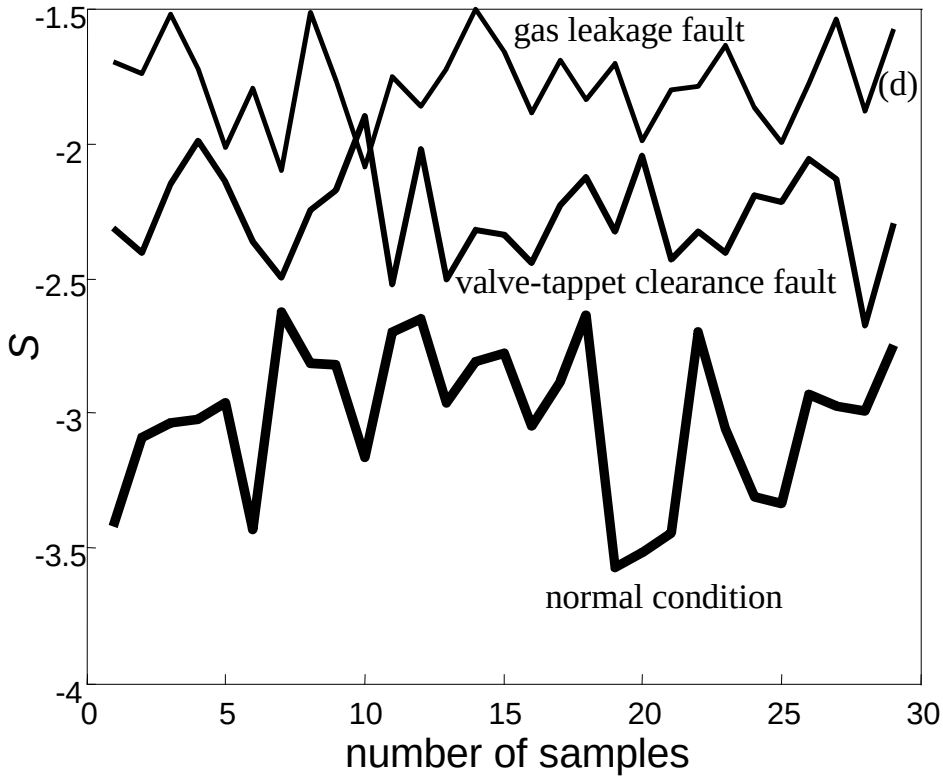
gas leakage fault
(d)
valve-tappet clearance fault
normal condition
S
number of samples

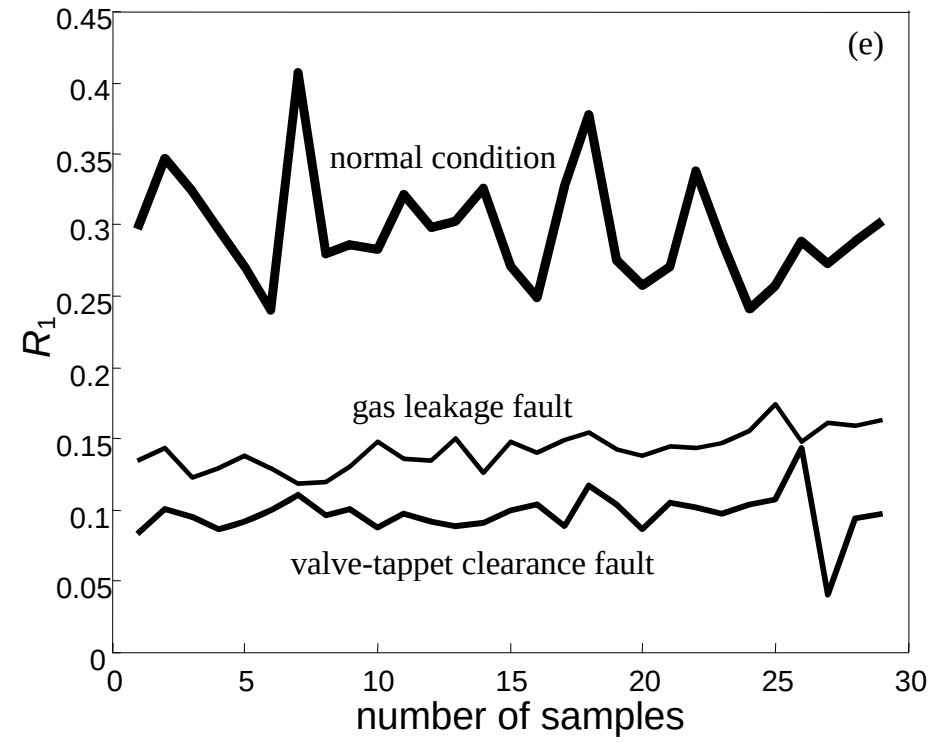

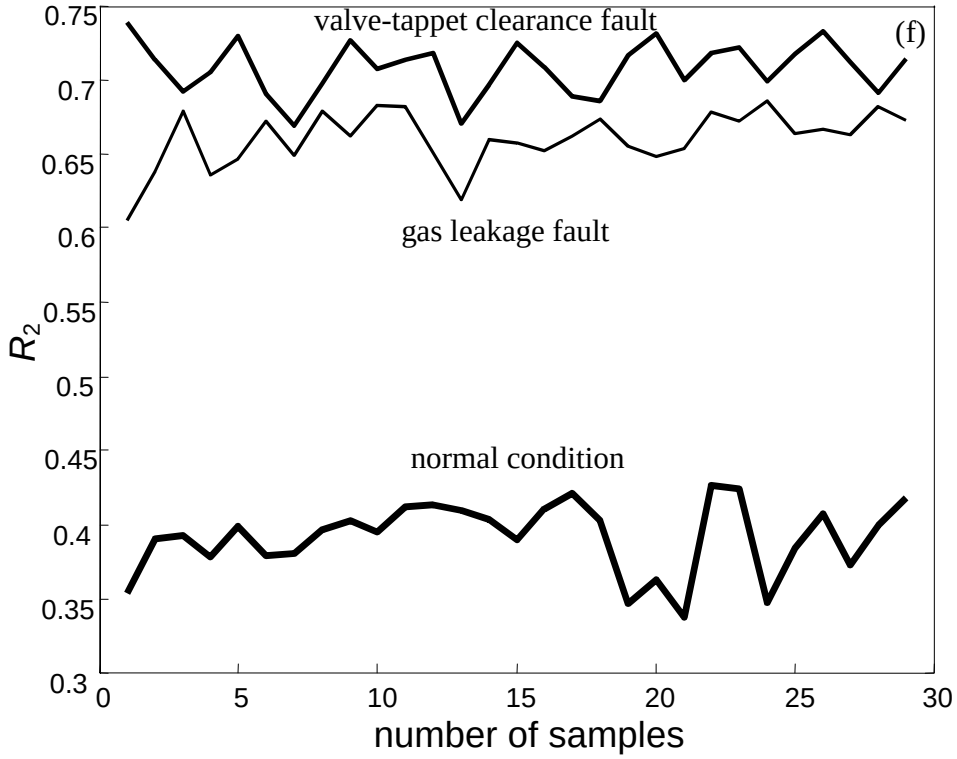

Fig.3 Computational results of the six vibratory criteria

(a) E_1 (b) E_2 (c) E_3 (d) S (e) R_1 (f) R_2

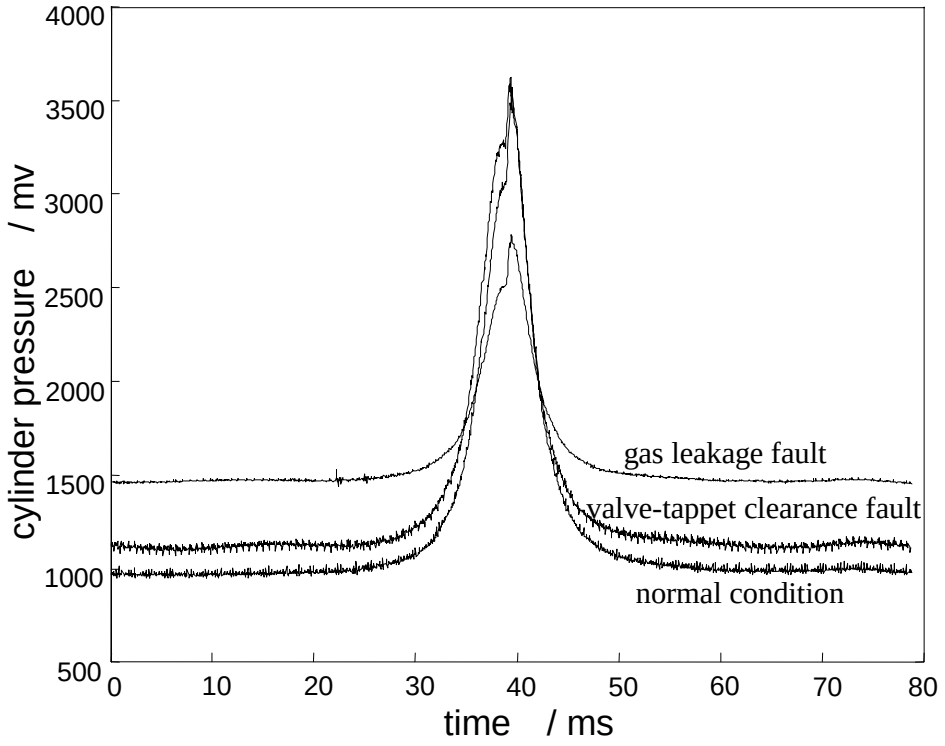

Fig.4 Cylinder pressure signals collected under different running conditions of the valve

(Drawn by W.-X. Yang)

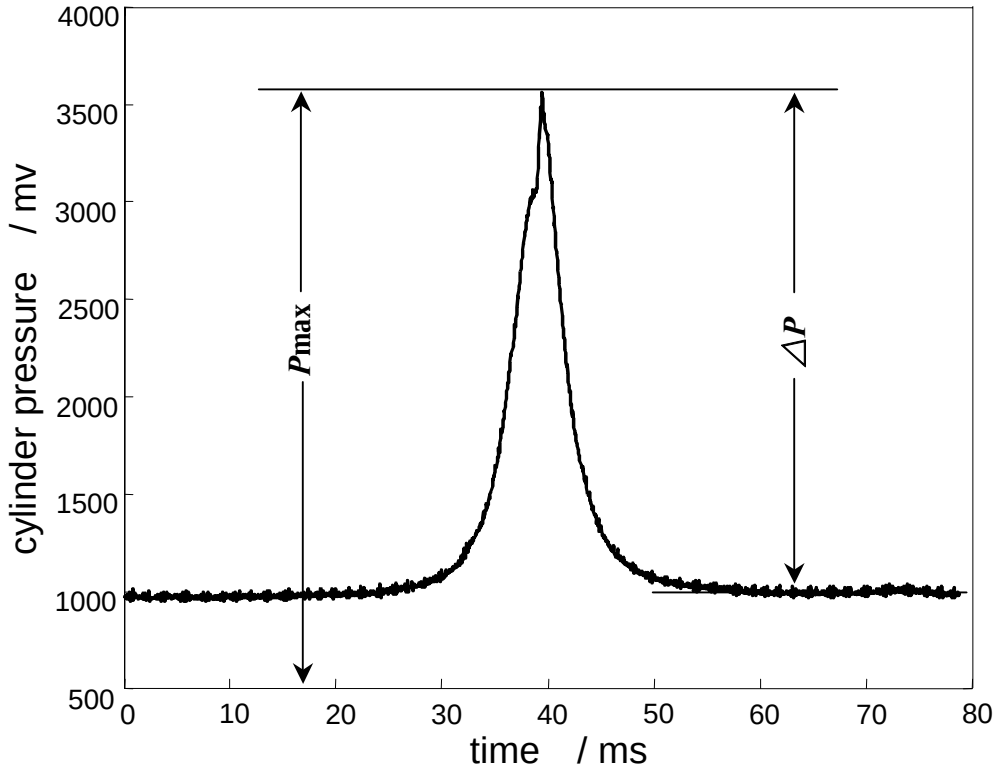

Fig.5 Cylinder pressure signatures P_{max} and ΔP

(Drawn by W.-X. Yang)

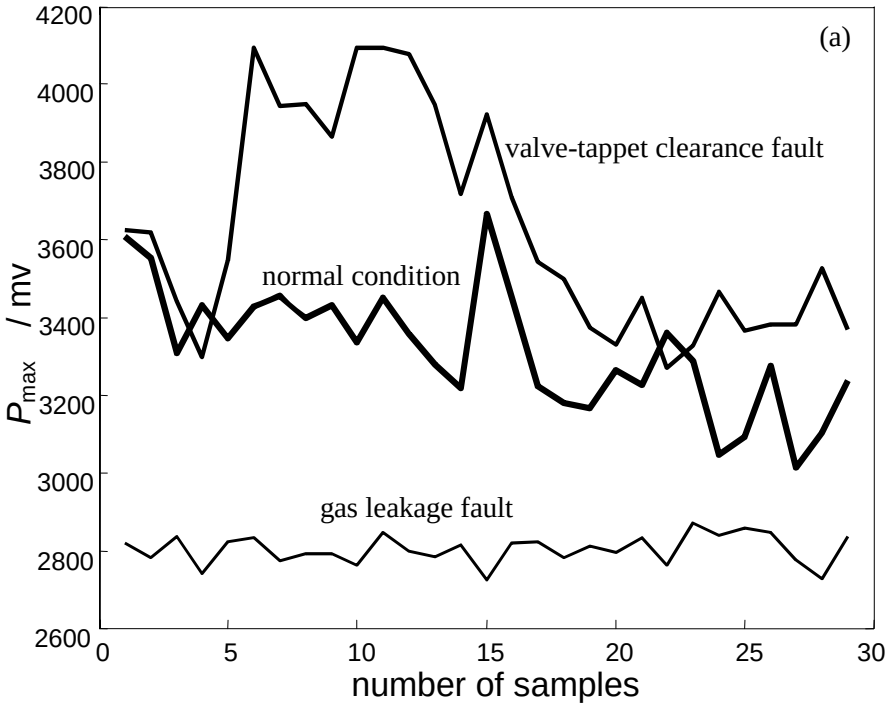

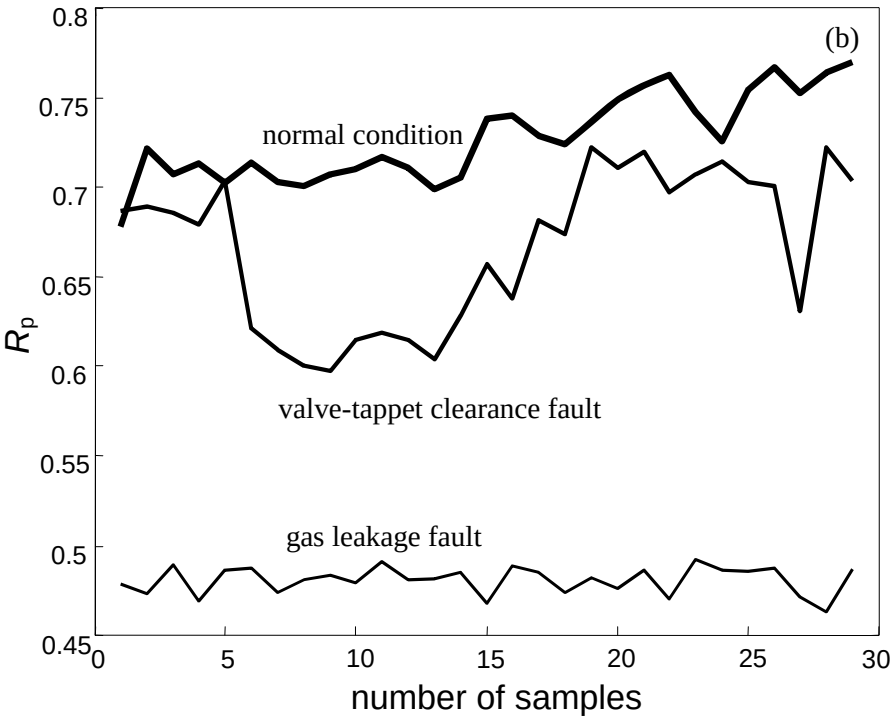

Fig.6 Calculation results of P_{max} and R_p

(a) P_{max} (b) R_p

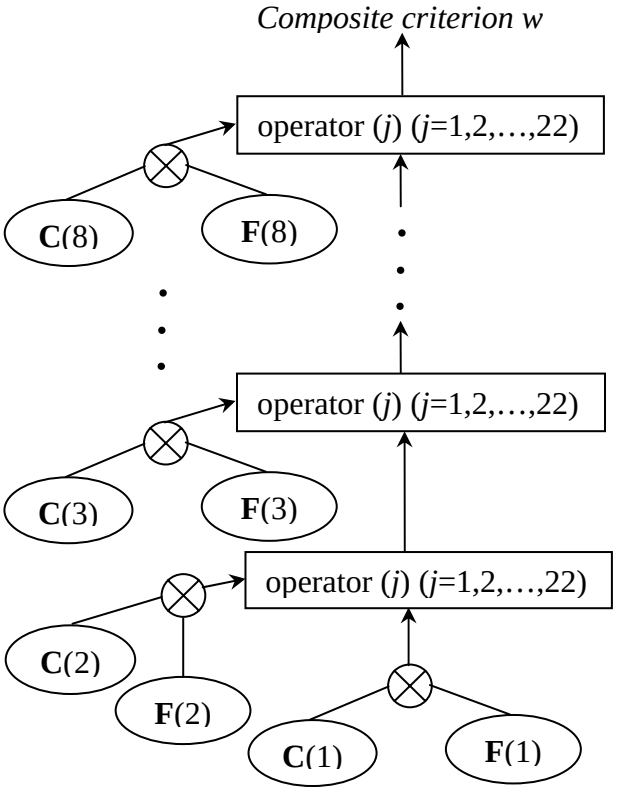

Fig.7 The diagram of the diagnosing tree

(Drawn by W.-X. Yang)

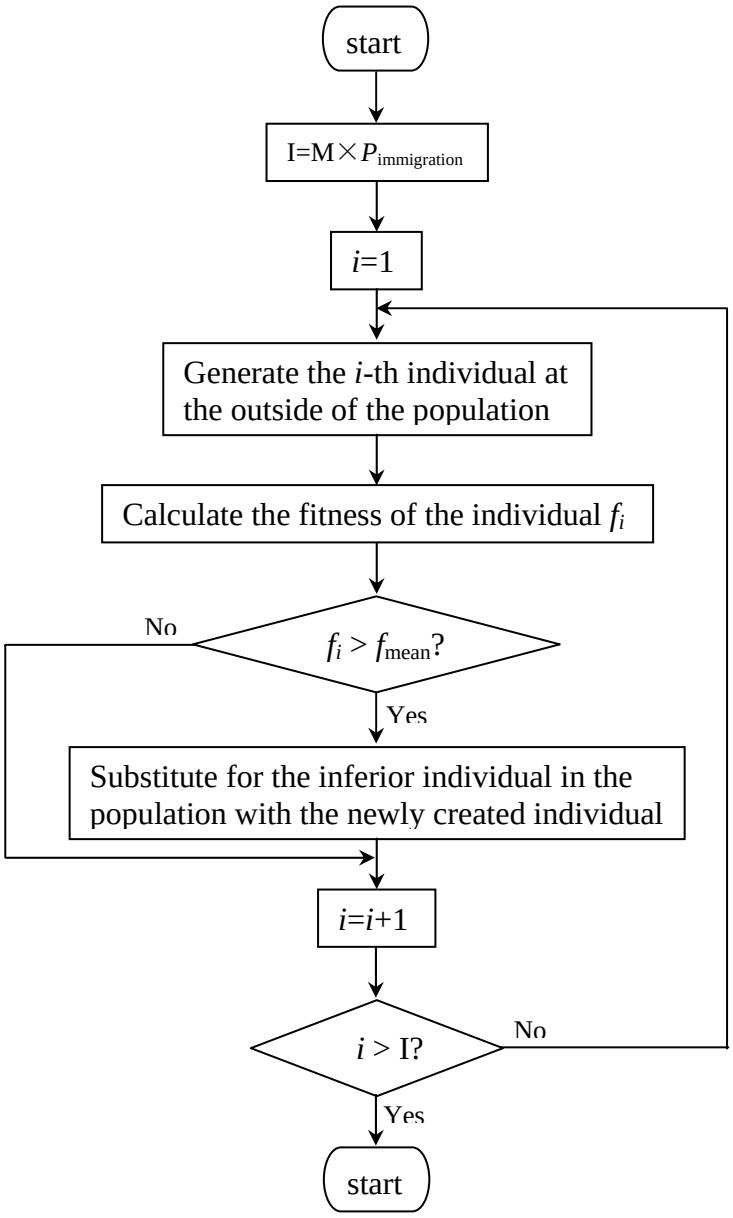

Fig. 8. The operating scheme of the IO

(Drawn by W.-X. Yang)

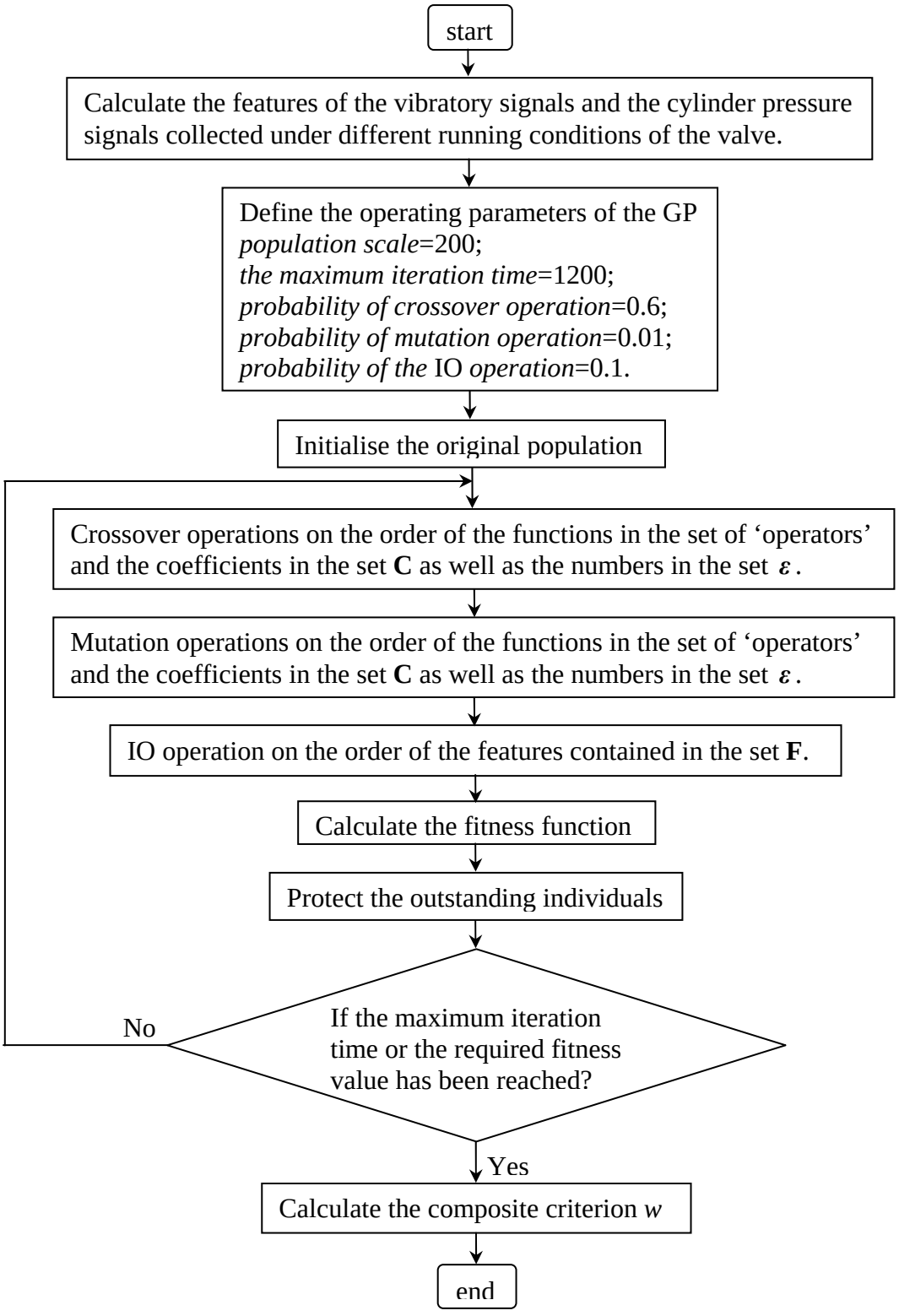

Fig.9 The operating diagram of the GP

(Drawn by W.-X. Yang)

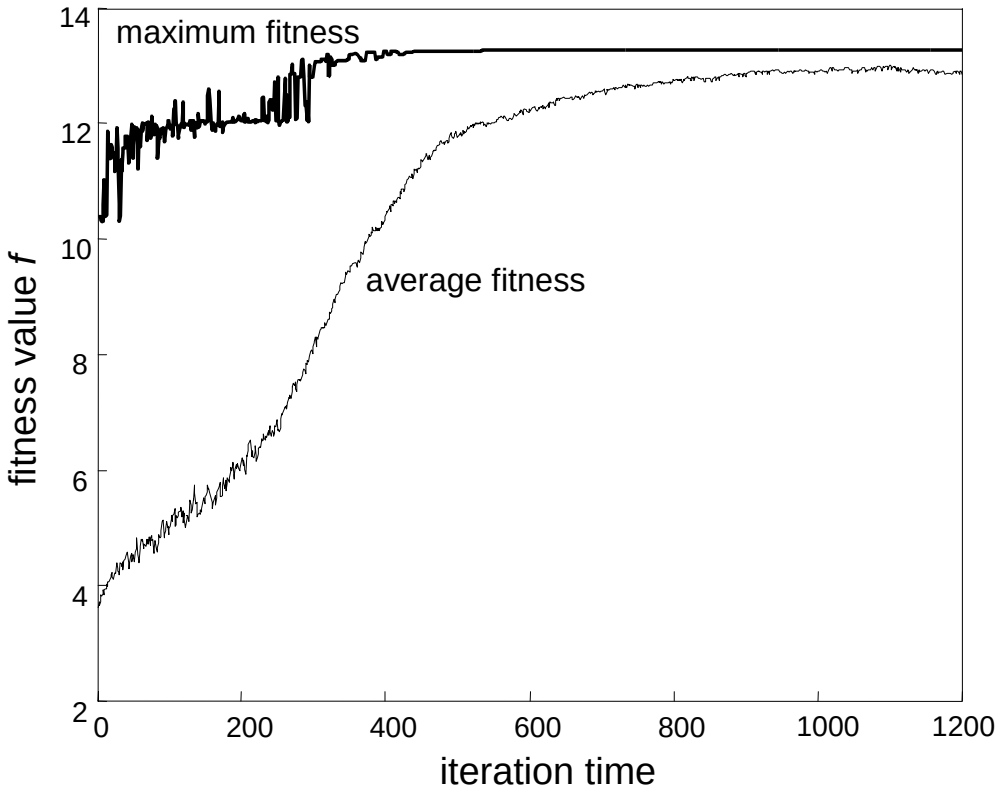

Fig.10 The recorded evolutionary history

(Drawn by W.-X. Yang)

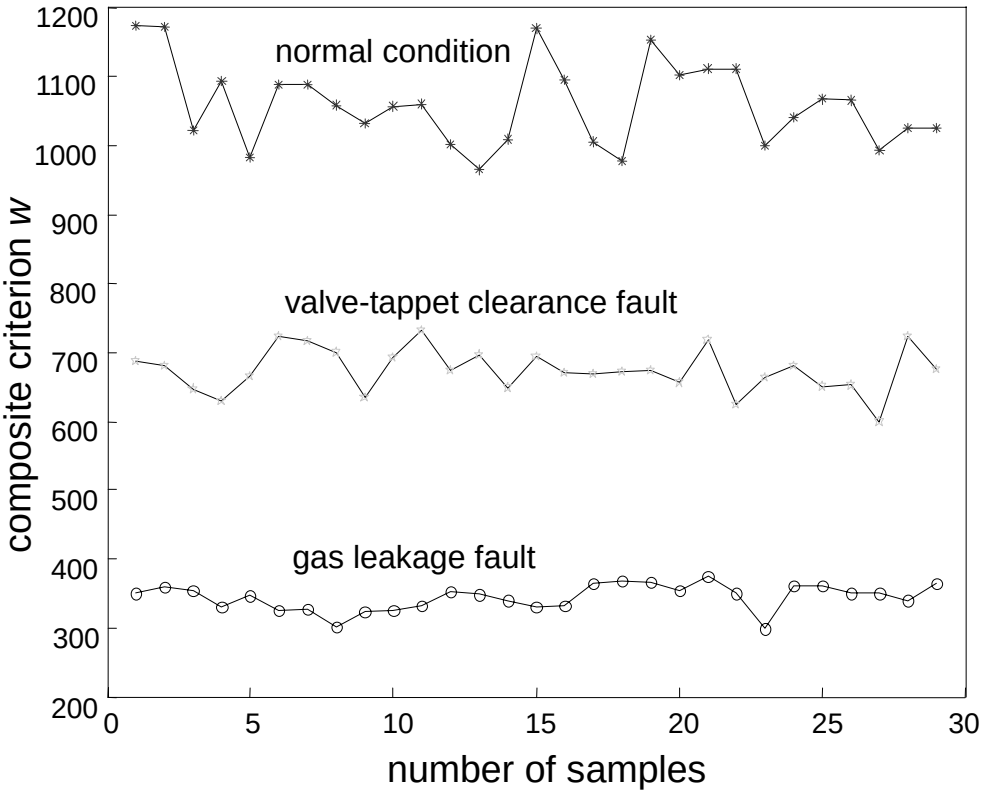

Fig.11 The results derived by the mathematical model

(Drawn by W.-X. Yang)

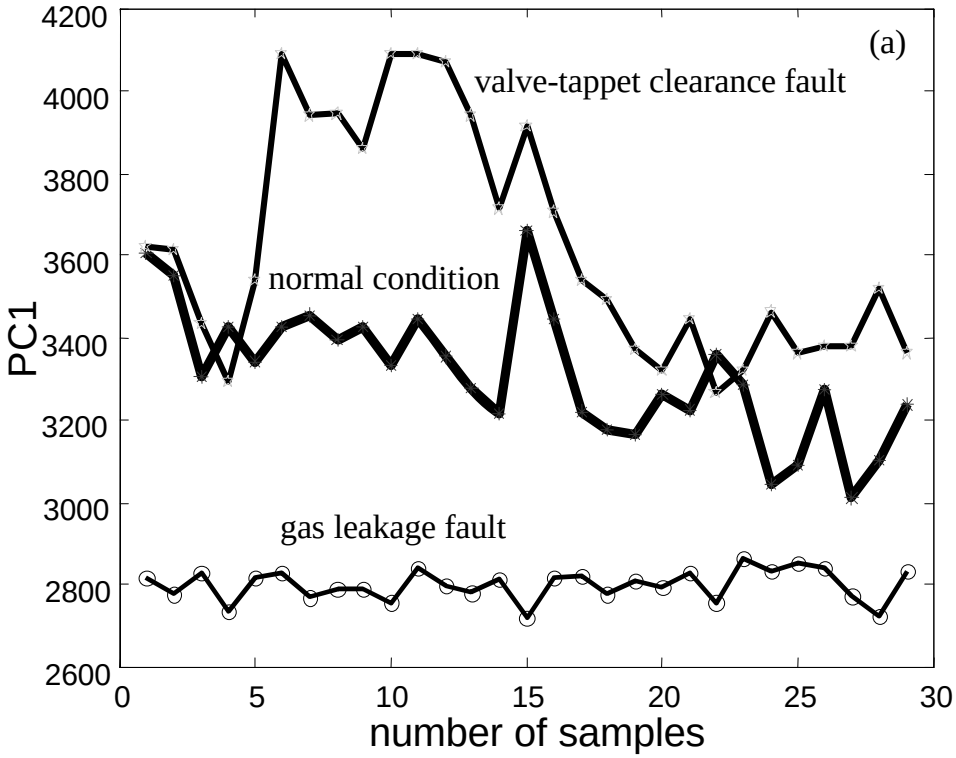
(a)
valve-tappet clearance fault
normal condition
gas leakage fault
PC1
number of samples
4200
4000
3800
3600
3400
3200
3000
2800
2600
0
5
10
15
20
25
30

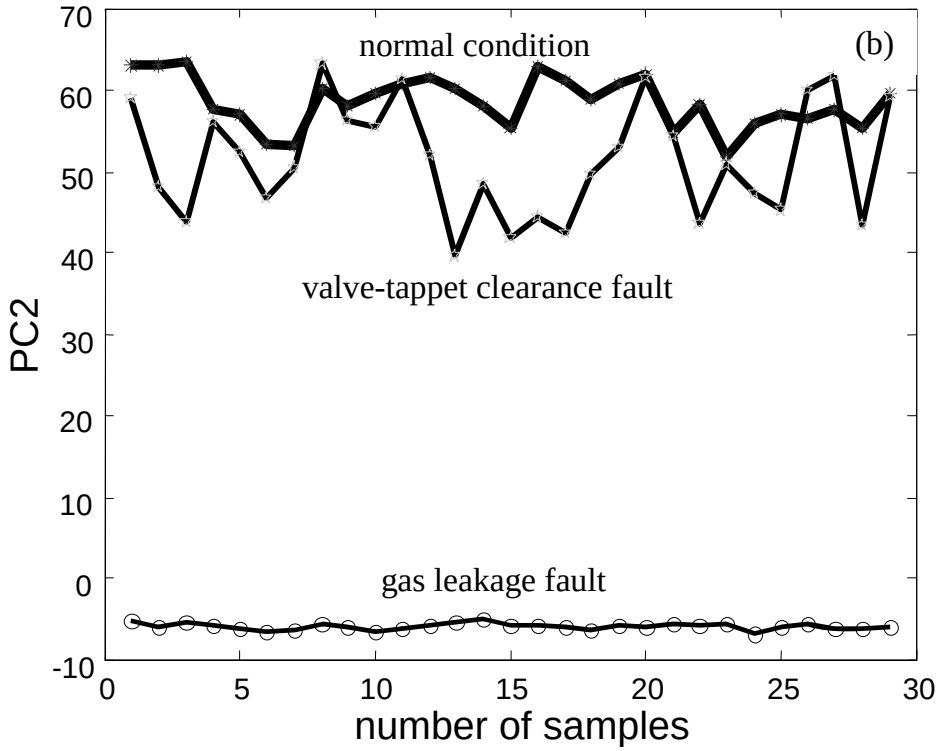
(b)
normal condition
valve-tappet clearance fault
gas leakage fault
PC2
number of samples
70
60
50
40
30
20
10
0
-10
0
5
10
15
20
25
30

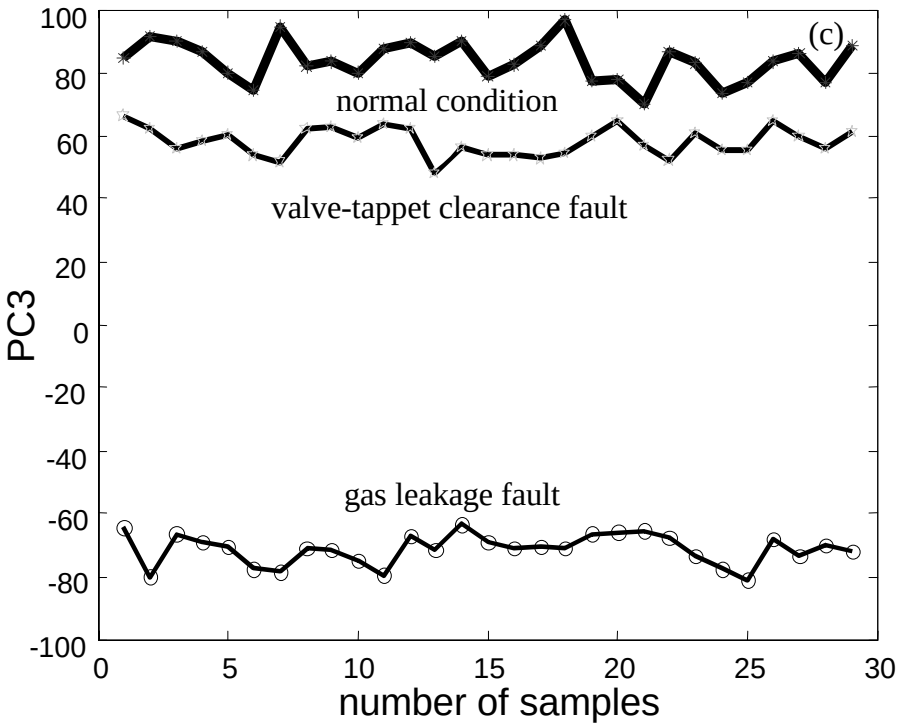

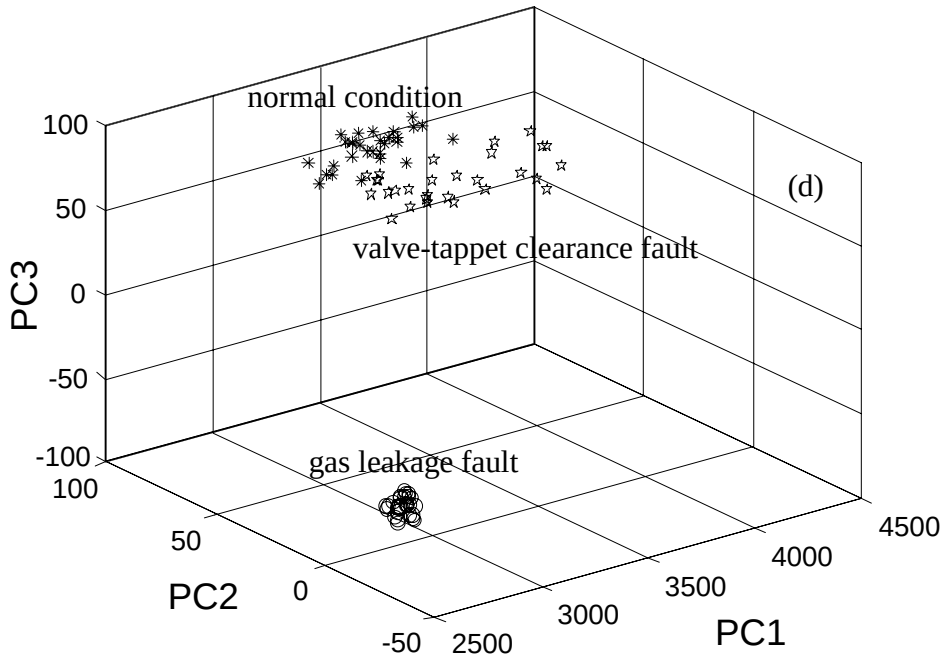

Fig.12 The results derived by the PCA method

(a) PC1 (b) PC2 (c) PC3 (d) Three dimensional plot PC1- PC2- PC3

Table 1 Mathematical functions

No.	Functions	No.	Functions
1	$y_{j+1} = c_i f_i + y_j$	12	$y_{j+1} = \sqrt{\lvert y_j / (\varepsilon_i + c_i f_i) \rvert}$
2	$y_{j+1} = c_i f_i - y_j$	13	$y_{j+1} = \sqrt{\lvert c_i f_i \rvert} + y_j$
3	$y_{j+1} = c_i f_i y_j$	14	$y_{j+1} = c_i f_i + \sqrt{\lvert y_j \rvert}$
4	$y_{j+1} = \lvert c_i f_i y_j \rvert$	15	$y_{j+1} = \sqrt{\lvert c_i f_i \rvert} - y_j$
5	$y_{j+1} = c_i f_i / (\varepsilon_i + y_j)$	16	$y_{j+1} = c_i f_i - \sqrt{\lvert y_j \rvert}$
6	$y_{j+1} = \sqrt{\lvert c_i f_i + y_j \rvert}$	17	$y_{j+1} = y_j \sqrt{\lvert c_i f_i \rvert}$
7	$y_{j+1} = \sqrt{\lvert c_i f_i - y_j \rvert}$	18	$y_{j+1} = c_i f_i \sqrt{\lvert y_j \rvert}$
8	$y_{j+1} = \sqrt{\lvert c_i f_i y_j \rvert}$	19	$y_{j+1} = \sqrt{\lvert c_i f_i \rvert} / (\varepsilon_i + y_j)$
9	$y_{j+1} = \sqrt{\lvert c_i f_i / (\varepsilon_i + y_j) \rvert}$	20	$y_{j+1} = c_i f_i / (\varepsilon_i + \sqrt{\lvert y_j \rvert})$
10	$y_{j+1} = y_j - c_i f_i$	21	$y_{j+1} = (c_i f_i)^2 + y_j$
11	$y_{j+1} = y_j / (\varepsilon_i + c_i f_i)$	22	$y_{j+1} = c_i f_i + y_j^2$

Table 2. Optimised results

Items	Optimised results
The order of the features in the set **F**	{1, 6, 2, 3, 5, 4, 8, 7}
The coefficients in the set **C**	{0.1526, 0.5351, 0.0212, 0.6745, 0.1540, 0.0515, 0.6745, 0.6745}
The constant numbers in the set $\boldsymbol{\varepsilon}$	{0.3647, 0.6619, 0.5746, 0.9965, 0.0279, 0.4955, 0.5746, 0.3860}
The order of the functions in the set of 'operators'	{8, 9, 10, 11, 20, 14, 5, 3}